2008

Purification and crystallization of a non-GluR2 AMPA-receptor ligand-binding domain: a case of cryo-incompatibility addressed by room-temperature data collection

Avinash Gill
Dartmouth College

Dean R. Madden
Dartmouth College

Acta Crystallographica Section F
Structural Biology and Crystallization Communications
ISSN 1744-3091

Avinash Gill and Dean R. Madden*

Department of Biochemistry, Dartmouth Medical School, 7200 Vail Building, Hanover, NH 03755, USA

Correspondence e-mail: drm0001@dartmouth.edu

Received 25 June 2008
Accepted 6 August 2008

Purification and crystallization of a non-GluR2 AMPA-receptor ligand-binding domain: a case of cryo-incompatibility addressed by room-temperature data collection

Glutamate is the major excitatory neurotransmitter in the brain. Among the cognate ionotropic glutamate receptors, the subfamily selective for AMPA (α-amino-3-hydroxy-5-methyl-4-isoxazole propionic acid) is responsible for most fast excitatory synaptic signaling and plays key roles in synaptic plasticity. AMPA receptors (AMPA-Rs) have also been implicated in a number of neurological disorders. To investigate subunit-specific differences in the ligand binding and activation of AMPA-Rs, the GluR4 AMPA-R ligand-binding domain (LBD) was crystallized in complex with full and partial agonists. This is the first non-GluR2 AMPA-R LBD available for structural analysis. Standard cryoprotection protocols yielded high-resolution diffraction from flash-cooled crystals of the complex with the full agonist glutamate. However, for cocrystals with the partial agonist kainate, systematic screening and optimization of cryoprotection conditions yielded at best mosaic, weak diffraction at 100 K. In contrast, room-temperature data collection from capillary-mounted kainate cocrystals exhibited reproducible diffraction to better than 3 Å resolution. Together, these crystals lay the foundation for a structural comparison of LBD–agonist interactions in distinct AMPA-R subunits.

1. Introduction

Glutamate-receptor ion channels are the principal mediators of excitatory synaptic signals in the central nervous system. They are classfied into subfamilies based on differential affinities for three characteristic ligands: α-amino-3-hydroxy-5-methyl-4-isoxazole propionic acid (AMPA), *N*-methyl-D-aspartic acid and kainic acid (KA). Of these, the AMPA receptors (AMPA-Rs) are the primary mediators of fast synaptic signals between neurons and also participate in regulating the strength of synaptic connections, a key foundation of learning and memory. Understanding the detailed mechanisms of AMPA-R activation and desensitization may thus provide insights into the stereochemical basis of these fundamental biological processes. AMPA-Rs have also been implicated in a number of neuropathologies (Dingledine *et al.*, 1999; Madden, 2002).

AMPA-Rs are assembled from the subunits GluR1–GluR4, usually as heteromeric combinations of two or more subunits. Although the subunits share high levels of sequence identity (68–73%), they exhibit distinct electrophysiological and pharmacological characteristics. As a result, the subunit-expression pattern of a given neuron can modulate its glutamatergic response *in vivo* (Dingledine *et al.*, 1999; Madden, 2002). Comparison of the stereochemistry of multiple AMPA-R subunits may help us to understand the basis of these functional differences and may also provide targets for the development of more subunit-specific pharmacological agents (Bräuner-Osborne *et al.*, 2000).

Functional diversity is provided by mechanisms of alternative splicing and RNA editing of the AMPA-R subunits. One of the most important modifications involves the RNA editing of a Gln codon to yield an Arg at a site in the ion-conduction pathway of the GluR2 subunit. AMPA-Rs lacking GluR2 subunits conduct both monovalent

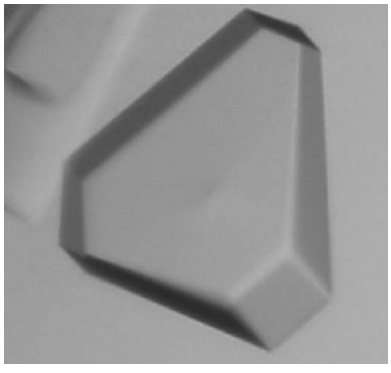

Table 1
Assessment of harvesting and mounting conditions for GluR4-LBD–KA cocrystals.

Condition†	Temperature (K)	Diffraction quality
HS‡ only	100	No spots
HS + 16–20% glycerol	100	No spots
HS + 24% glycerol	100	Few spots, ∼10–12 Å resolution
HS + 6–10% ethylene glycol	100	No spots
HS + 12–28% ethylene glycol	100	Few spots, ∼6–8 Å resolution
HS + 30% sucrose	100	Weak diffraction, ∼10–12 Å resolution
HS + 24% MPD	100	No spots
HS + 25–30% PEG 400	100	Weak diffraction, ∼8–10 Å resolution
HS + perfluoropolyether	100	No spots
HS/capillary†	∼293 (RT)	Strong diffraction, 2.2–3 Å resolution

† With the exception of the capillary-mounted crystal, all crystals were harvested in nylon loops and subjected to flash-cooling. ‡ Harvest solution (HS) corresponds either to the well solution used for crystallization or to the well solution supplemented with 1–2%(*w*/*v*) PEG as a potential stabilizer. For flash-cooling experiments, this was supplemented with various cryoprotectants at the concentrations listed.

cations and calcium, whereas AMPA-Rs incorporating GluR2 subunits are relatively impermeable to calcium. Both of these forms of AMPA-Rs are physiologically important (Cull-Candy *et al.*, 2006). In contrast, homomeric channels composed exclusively of edited GluR2 subunits have very low channel-conductance levels. Thus, while other AMPA-R subunits can form functional homomeric channels, edited GluR2 subunits cannot. Furthermore, ER retention mechanisms ensure that edited GluR2 subunits are not normally trafficked to the plasma membrane unless they assemble with other subunits to form heteromeric receptors (Greger & Esteban, 2007).

Despite these unique functional characteristics, GluR2 was the first iGluR subunit for which the LBD was crystallized (Armstrong *et al.*, 1998), and structures are now available for dozens of GluR2-LBD–ligand complexes. However, although crystal structures have since been determined for multiple members of the other iGluR subfamilies, GluR2 remains the only AMPA-R subunit to be crystallized to date (Oswald, 2004; Mayer, 2006). The available GluR2 LBD structures reveal a bilobate structure with an agonist-dependent cleft closure, the magnitude of which generally varies with the relative efficacy of the agonist (Madden, 2002). In contrast, analysis of the LBD of the NR1 subunit of the *N*-methyl-D-aspartate subfamily showed no such dependence (Inanobe *et al.*, 2005). Thus, in order to test the generality of the observations made with the GluR2 LBD, we have expressed, purified and crystallized the GluR4 LBD in complex with both a full and a partial agonist. In this report, we identify conditions that yield well ordered crystals for both protein–ligand complexes. Our studies also demonstrate the importance of assessing diffraction quality at room temperature for crystals that resist cryoprotection.

2. Materials and methods

2.1. Protein expression and purification

The *Rattus norvegicus* GluR4$_{flip}$ (UniProt accession No. P19493-2; Sommer *et al.*, 1990) LBD construct was generously provided by A. Birdsey-Benson. The 'S1' and 'S2' sequences (residues 393–507 and 633–775 of the mature sequence, respectively) were joined by a GT linker and subcloned into the pET16b vector (Novagen), which fused the sequence MG**HHHHHHHHHH**SSGHIEGRHM*LVPR*↓*GA*, containing a decahistidine tag (bold) and a thrombin cleavage site (italics; ↓ indicates the site of cleavage), to the N-terminus of the LBD-coding region and a single Ser residue to the C-terminus. The accuracy of the construct was verified by DNA sequencing.

XJb(DE3) Autolysis cells were transformed with the GluR4-LBD vector. 1 l SOC medium (with 3 m*M* L-arabinose and 100 µg ml^{-1} ampicillin) was inoculated with 5 ml of an overnight culture and incubated at 310 K. At an OD_{600} of ∼0.6, the cells were induced with 0.1 m*M* isopropyl *β*-D-1-thiogalactopyranoside, grown for 20 h at 293 K and harvested by centrifugation. Cell pellets were resuspended in 50 ml 20 m*M* Tris–HCl pH 8.0, 150 m*M* NaCl, 50 µg ml^{-1} lysozyme, 200 µg ml^{-1} sodium deoxycholate, ∼25 U ml^{-1} Benzonase (EMD) containing one Complete EDTA-free tablet (Roche). Cells were lysed by two freeze–thaw cycles (dry ice with EtOH/310 K water bath) followed in the case of residual turbidity by one pass through a French press at 6.9 MPa. The lysate was supplemented with 5 m*M* $MgSO_4$ and clarified by ultracentrifugation (45 min, 125 000*g*, 277 K). The supernatant was supplemented with 1 m*M* L-glutamate, 5 m*M* L-methionine, 1 m*M* phenylmethylsulfonyl fluoride and 5 m*M* imidazole and loaded onto a Qiagen Ni–NTA Superflow column pre-equilibrated with IMAC buffer (20 m*M* Tris–HCl pH 8.0, 150 m*M* NaCl, 1 m*M* sodium glutamate, 5 m*M* L-methionine) containing 5 m*M* imidazole. This column was then washed at 90 m*M* imidazole and eluted with a 90–400 m*M* imidazole gradient over eight column volumes in IMAC buffer. Eluates were pooled, concentrated and dialyzed in IMAC buffer containing 2 m*M* EDTA and then in 50 m*M* Tris–HCl pH 8.0, 75 m*M* NaCl, 10 m*M* $CaCl_2$ at 277 K.

The N-terminal His tag was removed using the Thrombin Clean-cleave kit (Sigma). Uncleaved protein was captured on a second metal-affinity column. Cleaved protein flowed through the column and was then dialyzed extensively (six buffer exchanges for 4 h each at a volume ratio of 200:1; 1 mg ml^{-1} protein concentration) against crystallization buffer (10 m*M* HEPES–NaOH pH 7.0, 30 m*M* NaCl, 1 m*M* EDTA). Protein concentrations were determined by Bradford assay (Bradford, 1976).

2.2. Crystallization

To prepare crystals of the glutamate complex GluR4-LBD–Glu, protein at 10 mg ml^{-1} was supplemented with L-glutamate to a final concentration of 10 m*M*. Crystals were obtained by vapor diffusion against Hampton Crystal Screen 1 condition No. 20 [25%(*w*/*v*) polyethylene glycol (PEG) 4000, 0.1 *M* sodium acetate pH 4.6, 0.2 *M* ammonium acetate] at 293 K in sitting drops (100 µl reservoir volume; 1:1 protein:buffer ratio in a total drop volume of 2 µl).

For crystallization of the kainate complex GluR4-LBD–KA, purified protein at 7 mg ml^{-1} was supplemented with kainate (Sigma) to a final concentration of 5 m*M*. GluR4-LBD–KA crystals grew in hanging drops (1:1 protein:buffer ratio in a total drop volume of 2 µl) equilibrated by vapor diffusion at 291 K against 500 µl 24–26%(*w*/*v*) PEG 1500, 50 m*M* sodium acetate pH 4.5–5.0.

2.3. Crystal harvest and mounting

GluR4-LBD–Glu crystals were soaked in crystallization buffer supplemented with 10 m*M* L-glutamate and 14%(*w*/*v*) glycerol as cryoprotectant and flash-cooled by plunging them into a liquid-nitrogen bath.

For the GluR4-LBD–KA crystals, varying concentrations of common cryoprotectants (Table 1) were tested for their ability to support vitrification of the harvest buffers [25–28%(*w*/*v*) PEG 1500, 50 m*M* sodium acetate pH 5.0, 5 m*M* kainate]. GluR4-LBD–KA crystals were either transferred directly into the final cryoprotectant solution or else transferred through increasing concentrations of cryoprotectant solution before flash-cooling in either liquid nitrogen or in the nitrogen stream of an Oxford Cryostream 700 at 100 K. Crystals were mounted for RT data collection in 0.5 mm glass

Table 2
Crystallographic and data-collection statistics.

Values in parentheses are for the highest resolution shell.

Protein	GluR4-LBD	GluR4-LBD
Ligand	L-Glutamate	Kainate
Conditions	100 K, cryocooled	RT, capillary mounted
Space group	$P2_1$	$C2$
Unit-cell parameters (Å, °)	a = 47.374, b = 105.124, c = 66.636, β = 97.26	a = 125.91, b = 48.75, c = 47.77, β = 109.06
Crystal dimensions (mm)	0.13 × 0.025 × 0.015	0.17 × 0.12 × 0.06
Matthews coefficient (Å^3 Da^{-1})	2.67	2.32
Molecules in ASU (Z)	2	1
Solvent content (%)	53.6	49.4
Resolution (Å)	19.51–1.85 (1.90–1.85)	11.95–2.7 (2.8–2.7)
Unique reflections	52938 (3988)	7353 (743)
Completeness (%)	96.4 (93.8)	95.6 (96.2)
$R_{\rm merge}$†	0.091 (0.182)	0.095 (0.241)
Mean redundancy	3.82 (3.80)	3.81 (3.84)
Mean $I/\sigma(I)$	11.37 (6.68)	11.14 (5.85)

† $R_{\rm merge} = \sum_{hkl}\sum_i |I_i(hkl) - \langle I(hkl)\rangle| / \sum_{hkl}\sum_i I_i(hkl)$.

capillaries (Hampton Research) using standard protocols (Rayment, 1985).

2.4. Data collection

Diffraction data were obtained on a MAR345dtb image-plate system (Rayonix) using Cu $K\alpha$ radiation from a rotating-anode generator (Rigaku) equipped with focusing optics (Genova). Crystals were screened for diffraction quality using 5–30 min 1° oscillation images. The GluR4-LBD–Glu data set was collected at 100 K (Oxford Cryostream 700) over a 180° oscillation range in 2 min 0.5° frames. The GluR4-LBD–KA data set was collected at RT over a 200° oscillation range in 3 min 1° frames.

2.5. Data analysis

The X-ray data sets obtained from GluR4-LBD–Glu and GluR4-LBD–KA crystals were analyzed using the *XDS* package (Kabsch, 1993). The *CNS* suite of programs (Brünger *et al.*, 1998) was used to perform rotation-function and translation-function searches from 12 to 3 Å resolution using the GluR2-LBD–Glu structure (PDB code 1ftj; sequence identity 89%) as the search model after modification using *CHAINSAW* to truncate non-identical side chains to the last common atom (Schwarzenbacher *et al.*, 2004).

3. Results

Here, we present conditions for the expression and purification of the LBD of the 'flip' splice isoform (Sommer *et al.*, 1990) of the GluR4 AMPA-R subunit ($\rm GluR4_{flip}$). The domain boundaries correspond to those of the S1S2J construct used previously in most crystallographic studies of the GluR2 LBD (Armstrong & Gouaux, 2000), which should facilitate direct comparison across subunits. Following purification, thrombin cleavage efficiently removes the polyhistidine tag (Fig. 1*a*).

Identification of crystallization conditions for both the glutamate (Fig. 1*b*) and kainate (Fig. 1*c*) complexes of the GluR4-LBD was straightforward. Glycerol was tested for its ability to support flash-cooling of the GluR4-LBD–Glu crystallization buffer. 14%(*w*/*v*) glycerol was found to be sufficient and GluR4-LBD–Glu crystals harvested into the corresponding cryobuffer exhibited excellent diffraction characteristics. A full data set was obtained on a rotating-anode source with a resolution limit of 1.85 Å ($R_{\rm merge}$ = 0.091; see Table 2).

In contrast, despite the optical quality of the GluR4-LBD–KA cocrystals, we were unable to identify cryoprotectant conditions that yielded high-resolution data following flash-cooling. A survey of the most common cryoprotectants identified several that permitted vitrification of the harvest buffer at the concentrations shown in Table 1. Crystals remained optically clear during transfer and following flash-cooling using both liquid nitrogen and cooled nitrogen gas. Nevertheless, the resulting diffraction patterns either showed no spots (26 of 48 crystals tested) or else exhibited blurry low-resolution diffraction (22 crystals) (Fig. 2*a*).

Given the simplicity of identifying cryoconditions for other GluR4-LBD crystals, we suspected that the GluR4-LBD–KA crystals were inherently disordered. However, to test this hypothesis, we mounted crystals in glass capillaries. Of 12 crystals, all exhibited diffraction extending to at least 4 Å and ten exhibited diffraction to better than 3 Å resolution (Fig. 2*b*). As a result, we were able to obtain a complete data set to a resolution of 2.7 Å ($R_{\rm merge}$ = 0.095; see Table 2).

Molecular-replacement searches carried out with the 1ftj GluR2-LBD search model yielded unambiguous solutions. Rotation and translation searches with the GluR4-LBD–Glu data set yielded two molecules in the asymmetric unit, with a correlation coefficient of 0.67 and a solvent content of 54%. Rotation and translation searches with the GluR4-LBD–KA data set yielded a single molecule in the

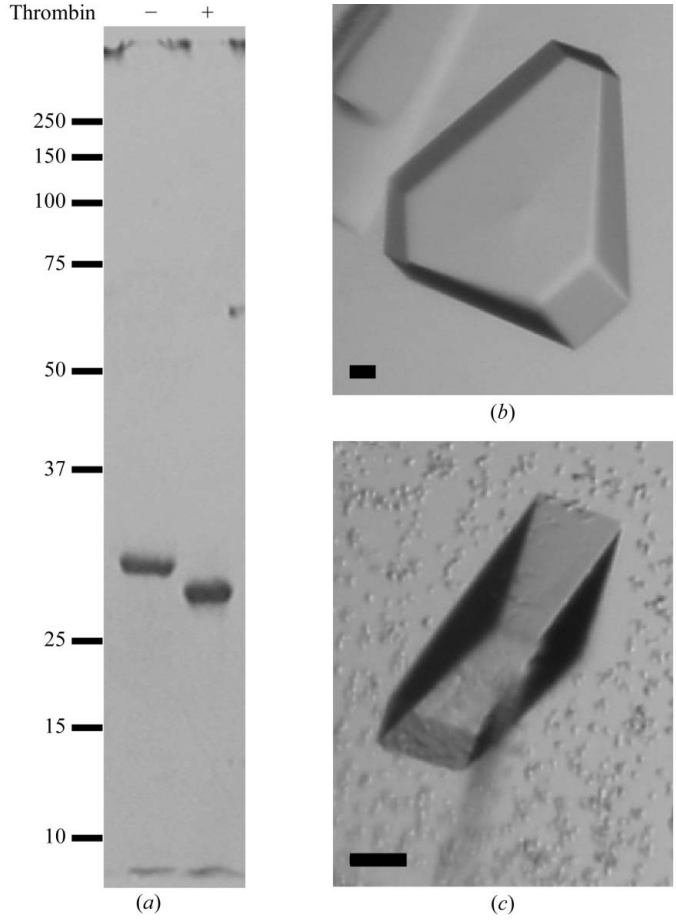

Figure 1
Protein purification and crystallization. (*a*) Silver-stained SDS–PAGE gel on which purified GluR4-LBD protein is resolved before (−) and after (+) thrombin cleavage and chromatographic removal of the polyhistidine tag. The positions of molecular-weight standards are shown on the left in kDa. Representative crystals are shown for the GluR4-LBD–Glu (*b*) and GluR4-LBD–KA (*c*) complexes. Scale bars are 25 µm.

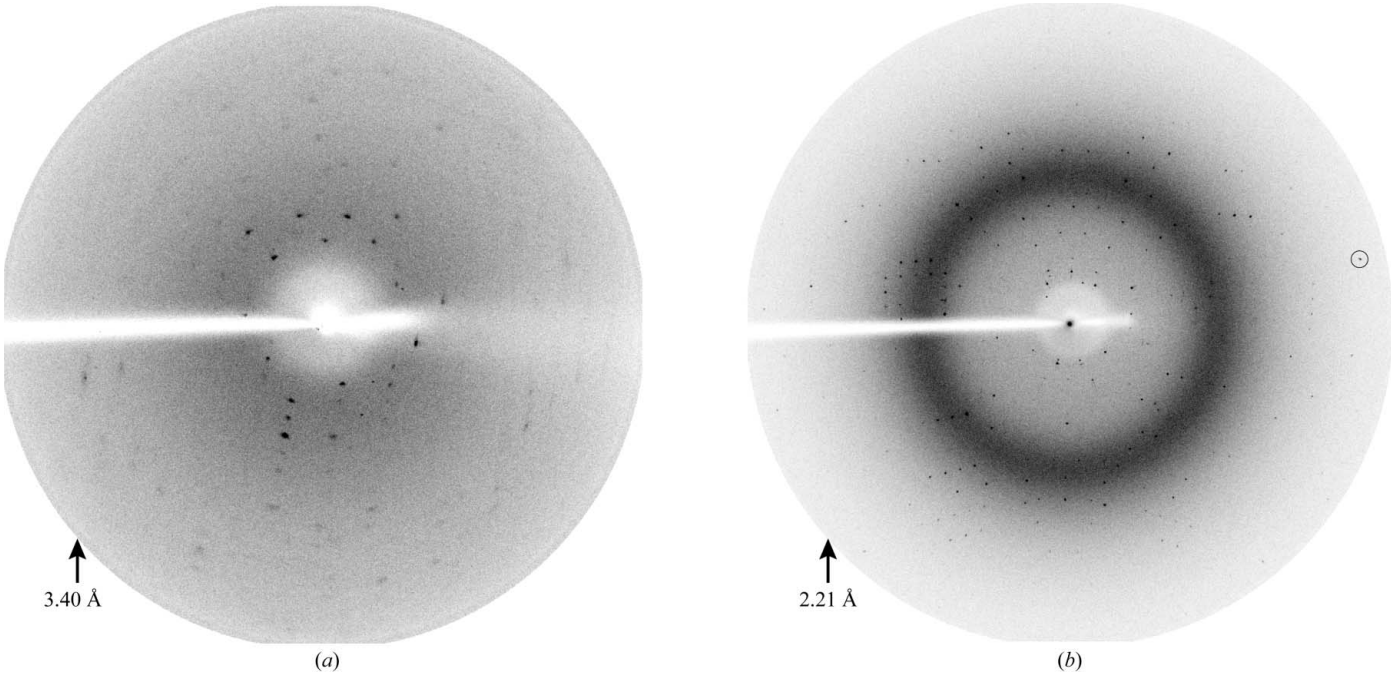

Figure 2
X-ray diffraction images of GluR4-LBD–KA cocrystals. (*a*) 10 min 1° oscillation image obtained at 350 mm crystal-to-image plate distance with a GluR4-LBD–KA cocrystal cryoprotected by soaking in harvesting buffer supplemented with 22% ethylene glycol and flash-cooled. Blurry spots were seen at low resolution and spots beyond 7 Å were difficult to distinguish from the background. (*b*) 3 min 1° oscillation pattern obtained at a crystal-to-image plate distance of 200 mm with a capillary-mounted GluR4-LBD–KA crystal. Well defined diffraction spots were visible at a resolution as high as 2.3 Å (black circle).

asymmetric unit, with a correlation coefficient of 0.73 and a solvent content of 49%.

4. Discussion

In this study, we have obtained high-resolution diffraction data for two complexes of the GluR4 AMPA-receptor LBD with full and partial agonists; this is the first non-GluR2 AMPA-R domain to be crystallized. We also report successful molecular-replacement solutions that provide the foundation for detailed crystallographic analysis. The determination of refined structures based on these data will permit a direct assessment of the extent to which the cleft-closure mechanism of channel activation, which has proposed for AMPA-Rs on the basis of GluR2-LBD structures alone, can be generalized to other subunits. It will also provide insights into the detailed agonist-binding stereochemistry of these physiologically important neurotransmitter receptors.

In the process, we encountered a situation that is not frequently described in the recent literature: a well ordered crystal for which systematic optimization of conditions failed to identify a cryoprotectant regime that preserves the order of the crystal lattice. Cryocrystallography has become so routine that it is sometimes assumed that failure to obtain high-resolution diffraction reflects an inherent lack of lattice order in the crystals, particularly if other crystals of the same protein have proven amenable to cryocrystallography. While we cannot exclude the possibility that further searching could identify successful cryoprotectant conditions for the GluR4-LBD–KA cocrystal, at this stage a common strategy would have been to initiate a search for alternative crystallization conditions. However, our experience underscores the importance of evaluating room-temperature diffraction characteristics before discarding cryo-incompatible crystals. Doing so enabled us to collect a high-resolution data set for the GluR4-LBD–KA cocrystal. The effort required is small compared with screening for alternative crystallization conditions, particularly using the novel methods that have been developed to facilitate capillary mounting (Basavappa *et al.*, 2003; Jeruzalmi, 2007). Thus, room-temperature data collection remains an important experimental option, despite the current near-ubiquity of cryocrystallographic techniques (Garman, 2003; Garman & Owen, 2006).

We would like to thank Amanda Birdsey-Benson for kindly providing the GluR4-LBD expression vector. We would also like to thank Athena Nomikos and Alexander Kivenson for assistance with protein expression and purification in the initial stages of the project. AG was supported by fellowships from the John Copenhaver and William Thomas Fellowship Fund and from the Rosaline Borison Memorial Fund. The research was support in part by a grant from the Hitchcock Foundation.

References

Armstrong, N. & Gouaux, E. (2000). *Neuron*, **28**, 165–181.
Armstrong, N., Sun, Y., Chen, G.-Q. & Gouaux, E. (1998). *Nature (London)*, **395**, 913–917.
Basavappa, R., Petri, E. T. & Tolbert, B. S. (2003). *J. Appl. Cryst.* **36**, 1297–1298.
Bradford, M. M. (1976). *Anal. Biochem.* **72**, 248–254.
Bräuner-Osborne, H., Egebjerg, J., Nielsen, E. O., Madsen, U. & Krogsgaard-Larsen, P. (2000). *J. Med. Chem.* **43**, 2609–2645.
Brünger, A. T., Adams, P. D., Clore, G. M., DeLano, W. L., Gros, P., Grosse-Kunstleve, R. W., Jiang, J.-S., Kuszewski, J., Nilges, M., Pannu, N. S., Read, R. J., Rice, L. M., Simonson, T. & Warren, G. L. (1998). *Acta Cryst.* D**54**, 905–921.
Cull-Candy, S., Kelly, L. & Farrant, M. (2006). *Curr. Opin. Neurobiol.* **16**, 288–297.
Dingledine, R., Borges, K., Bowie, D. & Traynelis, S. F. (1999). *Pharm. Rev.* **51**, 7–61.
Garman, E. (2003). *Curr. Opin. Struct. Biol.* **13**, 545–551.

Garman, E. F. & Owen, R. L. (2006). *Acta Cryst.* D**62**, 32–47.
Greger, I. H. & Esteban, J. A. (2007). *Curr. Opin. Neurobiol.* **17**, 289–297.
Inanobe, A., Furukawa, H. & Gouaux, E. (2005). *Neuron*, **47**, 71–84.
Jeruzalmi, D. (2007). *Methods Mol. Biol.* **364**, 43–62.
Kabsch, W. (1993). *J. Appl. Cryst.* **26**, 795–800.
Madden, D. R. (2002). *Nature Rev. Neurosci.* **3**, 91–101.
Mayer, M. L. (2006). *Nature (London)*, **440**, 456–462.
Oswald, R. E. (2004). *Adv. Protein Chem.* **68**, 313–349.
Rayment, I. (1985). *Methods Enzymol.* **114**, 136–140.
Schwarzenbacher, R., Godzik, A., Grzechnik, S. K. & Jaroszewski, L. (2004). *Acta Cryst.* D**60**, 1229–1236.
Sommer, B., Keinänen, K., Verdoorn, T. A., Wisden, W., Burnashev, N., Herb, A., Köhler, M., Takagi, T., Sakmann, B. & Seeburg, P. H. (1990). *Science*, **249**, 1580–1585.